Journal of Magnetics 11(1), 36-42 (2006)

Microstructure and Magnetic Properties of Au-doped Finemet-type Alloy

Anh-Tuan Le[1], Chong-Oh Kim[1], Nguyen Duy Ha[1], Nguyen Chau[2], Nguyen Duc Tho[2], and Heebok Lee[3]*

[1]*Research Center for Advanced Magnetic Materials, Chungnam National University, Daejeon 305-764, Korea*
[2]*Center for Materials Science, National University of Hanoi, 334 Nguyen Trai, Hanoi, Vietnam*
[3]*Department of Physics Education, Kongju National University, Kongju 314-701, Korea*

(Received 14 November 2005)

In this report, we demonstrate a comprehensive analysis of the effects of Au addition on the microstructure and magnetic properties of $Fe_{73.5}Si_{13.5}B_9Nb_3Au_1$ Finemet-type alloy. It was found that the as-quenched alloys were the amorphous state and turned into nanocrystalline state under heat treatments. The DSC analysis indicates that the sharply exothermal peak corresponding to the crystallization of the α-Fe(Si) was observed at 547-579°C depending on the heating rates, which is little higher than that of original Finemet (542-570°C, respectively). Besides, the thermomagnetic result confirmed that the full substitution of Cu by Au with the single phase structure in the $M(T)$ curve along cooling cycle. Ultrasoft magnetic properties of the nanocrystallized samples were significantly enhanced by the proper annealing such as the increase of permeability and the decrease of the coercivity. The optimum annealing condition was found at the annealing temperature of 540°C and the increase of the annealing time up to 90 min.

Key words : *microstructure, magnetic properties, annealing, thermomagnetic, nanocrystalline alloys*

1. Introduction

The $Fe_{73.5}Si_{13.5}B_9Nb_3Cu_1$ FINEMET alloy in its amorphous and nanocrystalline states has been extensively studied in the literature by various researchers [1-4]. This alloy has been found to exhibit excellent soft magnetic properties in its nanocrystalline state. Such nanocrystalline magnetic materials emerging from an amorphous matrix, by proper heat treatment, are significantly important since they are composed of different magnetic and structural phase, offering a wide range of applications. The FINEMET alloy is basically a Fe-Si-B amorphous alloy with Cu and Nb added to it. It has been reported that [2, 4] when it is given an optimal heat treatment from 773 to 818 K for an hour, it undergoes a transition into nanocrystalline state. This state has been identified as a two-phase structure in which ultrafine grains (10-20 nm) of the Fe-Si phase are embedded in an amorphous matrix essentially consisting of Fe, Nb, and B. The Fe-Si grains have been found dispersed into the amorphous matrix [5]. The quantity and the composition of the Fe-Si grains depend strongly on the thermal annealing condition of the alloy. The nonsolubility of Cu in Fe has been observed to increase the nucleation rate of the Fe-Si crystallites as Cu usually decreases the crystallization temperature and the small amount of Nb retards the growth of the size of the nuclei [6]. The nanosized Fe-Si grains have been found to be ferromagnetically exchange coupled through the Fe-Nb-B amorphous matrix. This was explained by Herzer *et al.* [7] using the random anisotropy model. According to this model, because these grains are smaller than the ferromagnetic exchange length (35 nm), magnetocrystalline anisotropy of the nanocrystalline phase averages out to zero. Thus, the FINEMET alloy exhibits high values of the saturation magnetization, permeability, and very low values of coercivity and high-frequency losses. The above combination of properties has become the driving force for a large number of studies reported on the present alloy. Additionally, the roles of elements in the FINEMET alloy for the nanocrystallization were also indicated. The Fe content is responsible for the excellent high saturation magnetization, the Si and B elements are added to promote glass formation in the precursor, while addition of Nb stabilizes the glassy phase that suppresses grain growth. Especially, the noble metal elements (i.e., Cu, Ag, and Au) serve as nucleating agents for the ferromagnetic nanocrystalline phase [1]. Recently, N. Chau *et al.* [8]

*Corresponding author: Tel: +82-41-850-8276,
Fax: +82-41-850-8271, e-mail: heebok@kongju.ac.kr

studied the crystallization process in FINETMET with Cu substituted by Ag of composition $Fe_{73.5}Si_{13.5}B_9Nb_3Ag_1$. It was pointed out that the crystallization of α-Fe(Si) phase has occurred strongly at higher temperature and higher crystallization activation energy than those of original FINEMET. However, the $M(T)$ curve measured along the cooling cycle showed that there was the multiphase structure in the sample. The substitution of Ag for Cu leads to the pinning of domain wall motion.

In the present work, therefore, with the hope of gaining some new rudimentary insights into the nature of the crystallization process, the microstructural changes, and into the magnetic characteristics of ultrafine FINETMET-type nanocrystalline magnetic materials, we thoroughly investigated the effects of Au addition on the microstructure and the magnetic properties of $Fe_{73.5}Si_{13.5}B_9Nb_3Au_1$ alloy. The correlations between the microstructure and the magnetic properties are discussed.

2. Experiment

Amorphous ribbon with nominal composition $Fe_{73.5}Si_{13.5}B_9Nb_3Au_1$ of about 8 mm in width and 20 μm in thickness were produced from ingots using the standard single copper wheel melt spinning technique. The $Fe_{73.5}Si_{13.5}B_9Nb_3Au_1$ nanocrystalline materials consisting of ultrafine grains embedded in an amorphous matrix were obtained by annealing their amorphous alloys at the temperatures of 530°C for 30 min, 60 min, and 90 min, of 540°C and 550°C for 30 min in vacuum.

The microstructure of the as-quenched amorphous ribbon and annealed ones was examined by X-ray diffraction (XRD Bruker D5005) with Cu-K_α radiation. Differential scanning calorimetry (DSC SDT 2960-TA Instruments) was used to examine the crystallization process of the as-quenched ribbons. A vibrating sample magnetometer (VSM DMS-880 Digital Measurement Systems) was used to measure magnetization as a function of the temperature for as-quenched alloy, with an applied field of 50 Oe and a heating/cooling rate of 4°C/min. An AC Permeagraph (AMH-410A, Walker) was employed to measure the room temperature permeability and coercivity of toroidal samples using the induction method.

The incremental permeability was measured along the ribbons axis under a dc longitudinal applied magnetic field. The samples with a length of about 15 mm were used for all measurements. The external dc field, applied by a solenoid, was swept through the entire cycle equally divided by 800 intervals from −300 Oe to 300 Oe. The schematic diagram of the experimental system can be found elsewhere [9, 10].

The permeability ratio (PR) can be defined as $\Delta\mu/\mu(\%) = 100\% \times [\mu(H) - \mu(H_{max})]/\mu(H_{max})$. where H_{max} is the maximum applied dc magnetic field. In present experiment H_{max}=300 Oe.

3. Results and Discussion

3.1. DSC and XRD analysis

First, we examined the microstructure of the as-quenched samples by using X-ray diffraction method. As can be seen in Fig. 1, the XRD pattern of as-quenched amorphous alloy exhibited only one broad peak around $2\theta = 45°$, which is often knows as a diffuse halo, indicating the amorphous nature of the as-quenched sample. Besides, the as-quenched alloy exhibits quite high plasticity and solidity higher than those of pure Finemet and the ribbon could be easy to bend [11].

A proper annealing regime for as-quenched amorphous alloys plays a decisive role in achieving the optimal soft magnetic properties [1]. We carried out DSC measurements in order to find out the most appropriate annealing temperature for as-quenched amorphous alloy composition. Figure 2 shows the DSC curves of the as-quenched amorphous alloy were performed with different heating rates from 10°C/min to 50°C/min. As can be seen clearly in Fig. 2, there were two exothermal peaks occurred in the crystallization process, the first one (547-579°C) depending on the heating rate from 10°C to 50°C/min corresponds to the nanocrystallization of the α-Fe(Si) soft magnetic phase and the second one (687-714°C) is related to the appearance of the boride-type phases (Fe_3B or Fe_2B) and recrystallization phenomena [12], which are

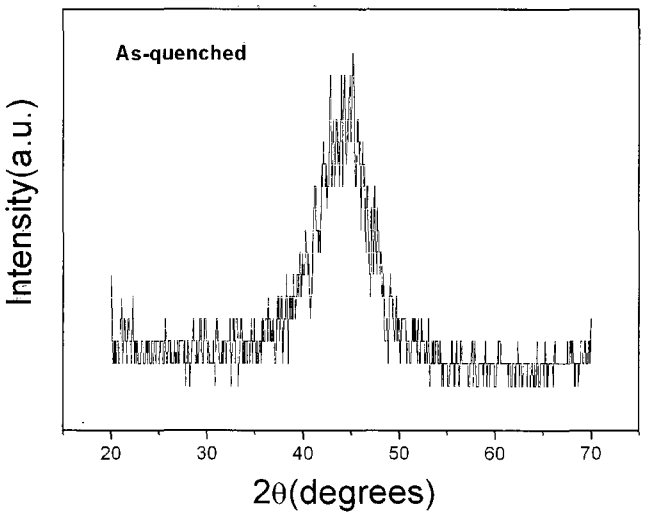

Fig. 1. The XRD pattern of as-quenched amorphous $Fe_{73.5}Si_{13.5}B_9Nb_3Au_1$ alloy.

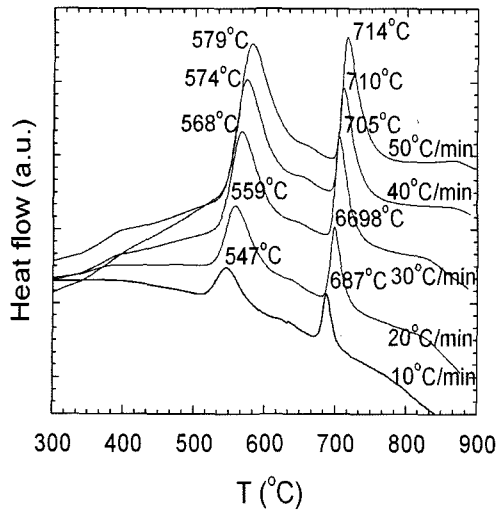

Fig. 2. The DSC curves of as-quenched $Fe_{73.5}Si_{13.5}B_9Nb_3Au_1$ alloy with different heating rates (from 10°C/min to 50°C/min).

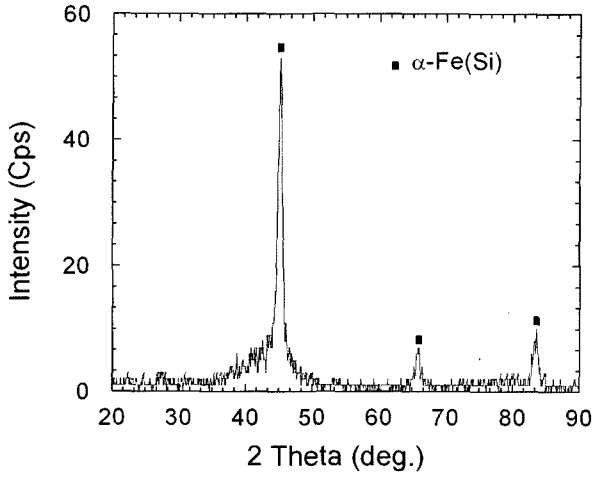

Fig. 3. The XRD pattern of the $Fe_{73.5}Si_{13.5}B_9Nb_3Au_1$ alloy annealed at 530°C for 90 min.

little higher than that of original Finemet (542-570°C and 686-719°C, respectively [13]). This result suggested that the substitution of Cu by Au has not changed the shape and peak position of DSC curves in comparison with that of pure Finemet indicating the Cu metal element is fully substituted by the Au element.

Based on the DSC results, the as-quenched amorphous ribbon was annealed at $T_a = 530$°C for 30 min, 60 min, and 90 min in vacuum in order to obtain the nanocrystalline samples with the ultra-fine α-Fe(Si) phase. Figure 3 shows, as an example, the XRD pattern of the sample annealed at 530°C for 90 min. As observed in Fig. 3, the XRD result confirmed that the crystallization of the ultrafine α-Fe(Si) phase occurred in the sample. This indicated that, upon a proper heat treatment, the as-

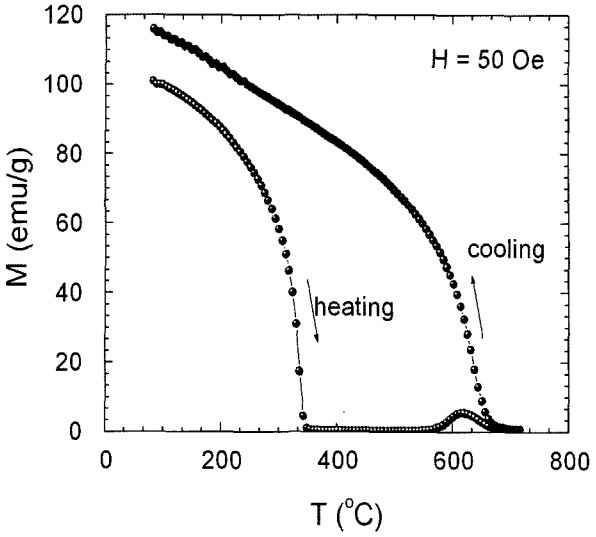

Fig. 4. Thermomagnetic curves of the $Fe_{73.5}Si_{13.5}B_9Nb_3Au_1$ amorphous alloy: (1) heating curve and (2) cooling curve.

quenched amorphous state transformed in to the bcc structure nanograins with excellent soft magnetic properties. Furthermore, the particle size, d, of α-Fe(Si) grains can be determined from the breadth, B, of the X-ray diffraction peak, according to the Scherrer expression [14]:

$$d = \frac{0.9\lambda}{B\cos\theta_B} \quad (1)$$

Where λ is the X-ray wavelength (λ = 1.54056 Å), θ is the diffraction angle, and B is the full width at half maximum (FWHM). Our calculations from the XRD pattern according to Eq. (1) revealed that the mean grain size of crystallites is about 10.8 nm which is less than the ferromagnetic exchange interaction length as reported in Finemet alloy (~35 nm) [13].

3.2. Magnetic characteristics

3.2.1. Thermomagnetic analysis

Next, the crystallization kinetics of the as-quenched amorphous alloy was examined by the thermomagnetic curve with heating and cooling cycles as displayed in Fig. 4. It can be seen that, as the temperature increased, the magnetization was abruptly reduced marking the Curie temperature of the amorphous phase (T_{c1}) (see the heating curve in Fig. 4). With further increasing temperature, the magnetization is small and nearly constant over a large temperature interval up to a region of onset temperature, in which the crystallization of α-Fe(Si) soft magnetic phase occurred leads to an increase of the magnetization and quickly reached a maximum, then again rapidly

decreased at high temperatures. In the cooling process with decreasing temperature (see the cooling curve in Fig. 4), a large amount of α-Fe(Si) grains are crystallized in the sample leading to a strong increase of the magnetization. From the $M(T)$ curve, we determined three Curie temperatures of the different phases: T_{c1}- the Curie temperature of the initial amorphous phase, T_{c2}- the Curie temperature of the remaining amorphous matrix, and T_{c3}- the Curie temperature of the nanocrystalline phase, respectively. Note that T_{c3} was determined from the cooling cycle of the thermomagnetic curve. As observed in Fig. 4, it is worth mentioning that the single phase structure in the $M(T)$ curve along cooling cycle was observed, whereas in the case of Ag substituted for Cu in Finemet alloy the multiphase structure was occurred [8].

3.2.2. Effect of annealing time and temperature on the magnetic softness

In fact, the crystallization of magnetic phases originating from the diffusion effect of different atoms existing in the alloys and the diffusion depends on the heating temperature as well as the temperature keeping time [13]. In this regard, we first investigated the influences of annealing time on the soft magnetic properties of alloy.

The amorphous alloys were annealed at the temperature of 530°C for 30 min, 60 min, and 90 min in vacuum. After that, the amorphous and nanocrystalline samples were examined by the magnetic hysteresis loops. Figure 5 shows, as an example, the hysteresis loops of the as-quenched amorphous alloy and annealed at 530°C for 90 min. As observed in Fig. 5, the hysteresis loop of the amorphous alloy showed the squared hysteresis loop. This

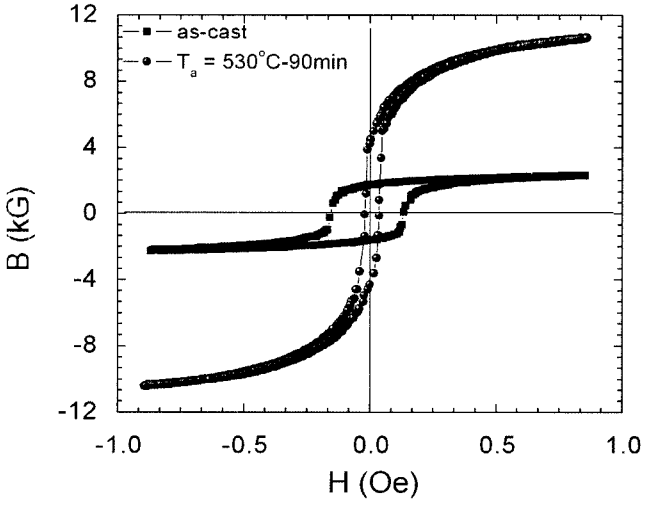

Fig. 5. Magnetic hysteresis loops of the $Fe_{73.5}Si_{13.5}B_9Nb_3Au_1$ sample (both as-quenched and annealed at 530°C for 90 min).

Table 1. Magnetic characteristics of the as-quenched $Fe_{73.5}Si_{13.5}B_9Nb_3Au_1$ alloy and annealed at 530°C for different annealing time.

Sample	μ_i	μ_{max}	H_c (Oe)	M_s (emu/g)	B_{max} (kG)
As-quenched	1,300	6,900	0.144	127	2.3
T_a=530°C for 30 min	13,000	50,000	0.036	144	8.5
T_a=530°C for 60 min	15,000	62,000	0.024	151	10.1
T_a=530°C for 90 min	19,000	99,000	0.022	167	10.7

is likely related to the magnetoelastic anisotropy distribution due to the stress induced during the fabrication process. However, the hysteresis loop of the annealed sample has a typical form with improved soft magnetic properties. Accordingly, the magnetic characteristics of all samples also were summarized in Table 1. It can be seen clearly that the initial permeability, the maximum permeability, the saturation magnetization, and the maximum flux density increased with increasing annealing time, while the coercivity decreased. This is likely attributed to an increase of the crystallization volume fraction of the α-Fe(Si) phase with increasing annealing time, thus leading to the ultrasoft magnetic properties (see Table 1) in the sample caused by the strongly magnetic exchange coupling between the grains. In order to confirm this, based on DSC measurement and using a method proposed recently by Leu and Chin [15] to determine the crystallization volume fraction (c_f) of the α-Fe(Si) phase:

$$\chi_f = \frac{\Delta H_a - \Delta H_t}{\Delta H_a} \tag{2}$$

where ΔH_a and ΔH_t are the crystallization enthalpy of the as-quenched amorphous alloy and the alloy annealed at a given temperature for time t, respectively.

Indeed, according to Eq. (2), we derived the crystallization volume fraction (χ_f) of the α-Fe(Si) phase for the samples annealed at 530°C for 30 min, 60 min, and 90 min to be 73%, 78%, and 84%, respectively. This result was good in agreement with the explanation as mentioned above.

In order to further elucidate the influences of annealing time on the soft magnetic properties of alloys. Simultaneously, we measured the PR curves as a function of longitudinal dc external magnetic field at various frequencies up to 5 MHz for the as-quenched alloy and annealed ones as displayed in Fig. 6. As can be seen in Fig. 6, the PR curves exhibit a maximum peak at zero field (H_{dc} = 0), the magnitude of PR decreases with increasing frequency while the shape of the PR curves becomes broader. Among the samples investigated, the nanocrystalline sample

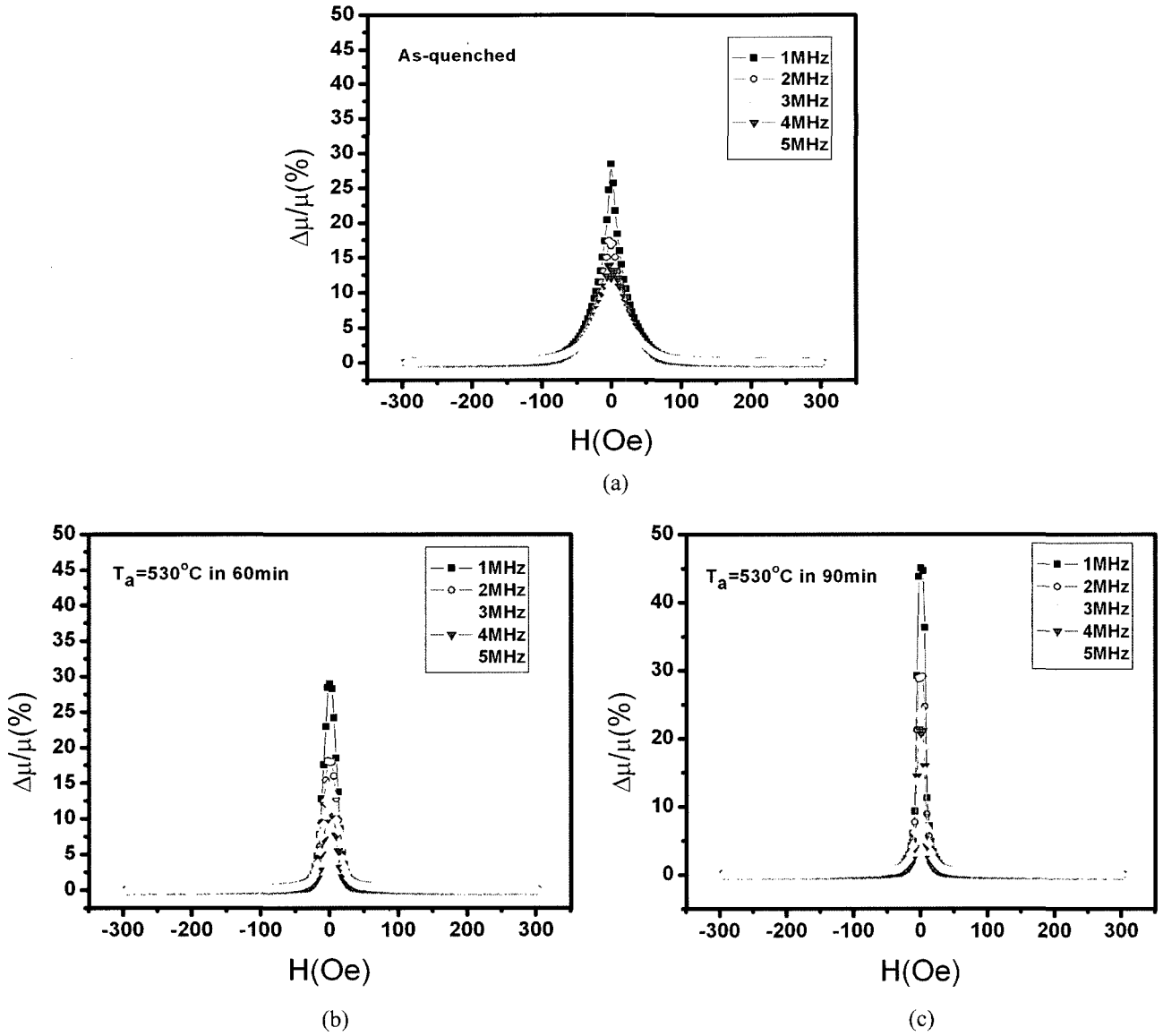

Fig. 6. PR curves measured as a function of the external magnetic field at various frequencies for the (a) as-quenched alloy, ones annealed at (b) 530°C for 60 min, and (c) 530°C for 90 min.

annealed at 530°C for 90 min exhibits the largest maximum value of PR ($\Delta\mu/\mu_{max}(\%)$), and the largest sharpness (see Fig. 6c) which is mainly due to the ultrasoft magnetic properties in this sample. This together with the results obtained from the magnetic hysteresis loops revealed that, with increasing annealing time up to 90 min, the crystallization of α-Fe(Si) phase was detected in all the samples investigated. It is evident that, upon annealing time, the as-quenched amorphous state transformed into the ultra-fine nanograins with excellent soft magnetic properties.

Finally, to complete the analysis, we examined the influences of annealing temperature on the soft magnetic properties of alloys by the mean of the permeability measurement. Figure 7 shows the PR curves as a function of longitudinal dc external magnetic field measured at various frequencies from 1 MHz to 5 MHz for the samples annealed at 530°C, 540°C and 550°C for 30 min, respectively. As can be seen in Fig. 7, among the temperatures investigated, the nanocrystalline sample annealed at 540°C for 30 min exhibits the largest maximum value of PR ($\Delta\mu/\mu_{max}(\%)$) and the largest sharpness of the curve shape indicating the largest magnetic softness in the sample (see Fig. 7b). This is likely ascribed to the microstructural changes caused by proper annealing, i.e., the appearance of nanoscale α-Fe(Si) grains where magneto-

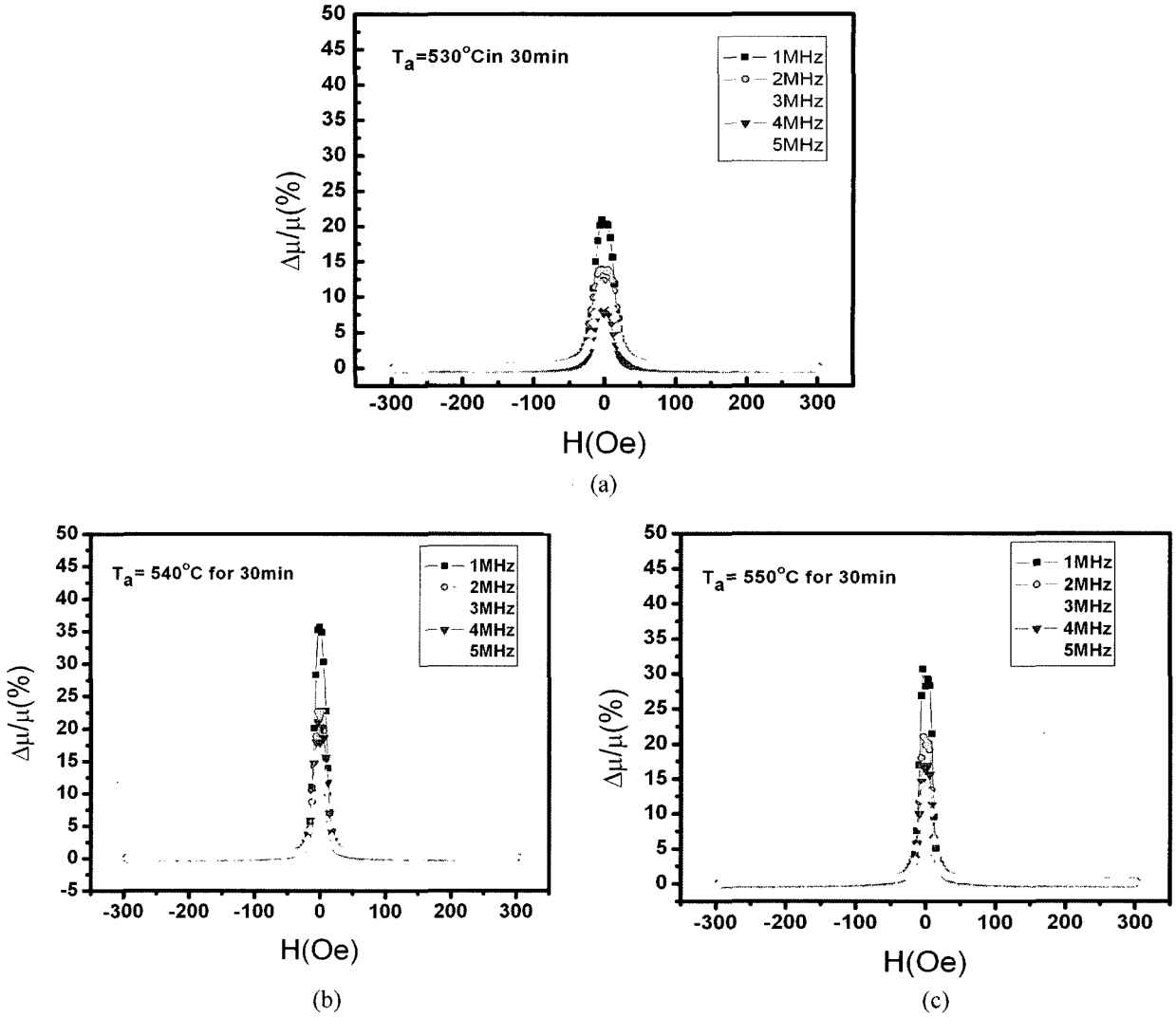

Fig. 7. PR curves measured as a function of the external magnetic field at various frequencies for different annealing temperatures, annealed at (a) 530°C, (b) 540°C, and (c) 550°C for 30 min.

crystalline anisotropies are averaged out, therefore nanocrystalline grains are strongly coupled though magnetic exchange interactions, thus leading to the ultrasoft magnetic properties.

4. Conclusions

The effects of Au addition on the microstructure and the magnetic properties of $Fe_{73.5}Si_{13.5}B_9Nb_3Au_1$alloy have been thoroughly investigated and the following conclusions obtained:

a) The as-quenched amorphous alloy exhibits quite high plasticity and solidity higher than those of original Finemet and the ribbon could be easy to bend.

b) With increasing annealing time, the crystallization of the ultrafine α-Fe(Si) phase occurred and resulted in the increase of the crystallization volume fraction of nanocrystalline phase.

c) Thermomagnetic analysis shows that the single phase structure in the $M(T)$ curve along cooling cycle was observed. This suggests that the Cu element can be well substituted by the Au element.

d) Ultrasoft magnetic properties (i.e., the increase of permeability, and maximum flux density as well as the decrease of the coercivity) of the nanocrystalline samples were found by optimum annealing condition, i.e., the annealing temperature of 540°C and the increase of the annealing time up to 90 min.

Acknowledgments

The authors wish to acknowledge the Center for

Materials Science, National University of Hanoi (Vietnam) kindly supplied the samples. This work was supported by Korean Science and Engineering Foundation through Research Center for Advanced Magnetic Materials at Chungnam National University.

References

[1] M. E. McHenry, M. A. Willard, and D. E. Laughlin, Prog. Mater. Sci. **44**, 291 (1999).
[2] Y. Yoshizawa, S. Oguma, and K. Yamauchi, J. Appl. Phys. **64**, 6044 (1988).
[3] M. Ohnuma, D. H. Ping, T. Abe, H. Onodera, K. Hono, and Y. Yoshizawa, J. Appl. Phys. **93**, 9186 (2003).
[4] P. Martin, M. Lopez, A. Hernando, Y. Iqbal, H. A. Davies, and M. R. J. Gibbs, J. Appl. Phys. **92**, 374 (2002).
[5] R. S. Tutelli, V. H. Duong, R. Grossinger, M. Schwetz, E. Ferrara, and N. Pillmayr, IEEE Trans. Magn. **36**, 508 (2000).
[6] J. D. Ayers, V. G. Harris, J. A. Sprague, and W. T. Elam, J. Appl. Phys. **64**, 974 (1994).
[7] G. Herzer, IEEE. Trans. Magn. **25**, 3327 (1989).
[8] N. Chau, N. Q. Hoa, and N. H. Luong, J. Magn. Magn. Mater. **290**, 1547 (2005).
[9] Heebok Lee, Y. K. Kim, K. J. Lee, and T. K. Kim, J. Magn. Magn. Mater. **215**, 310 (2000).
[10] Heebok Lee, Y. K. Kim, T. K. Kim, and S. C. Yu, J. Magn. Magn. Mater. **215**, 307 (2000).
[11] N. Chau, N. Q. Hoa, N. D. The, L. V. Vu, and T. M. Thang, Proceeding of the Eighth German-Vietnamese on Physics and Engineering, Erlangen, April 03-08, 2005.
[12] M. H. Phan, H. X. Peng, M. R. Wiscom, S. C. Yu, and N. Chau, Composites, Part A (inpress).
[13] N. Chau, N. X. Chien, N. Q. Hoa, P. Q. Niem, N. H. Luong, N. D. Tho, and V. V. Hiep, J. Magn. Magn. Mater. **282**, 174 (2004).
[14] B. D. Cullity, Elements of X-ray diffraction, 2nd Ed, Addison-Wesley Publishing Company, Inc., Reading, MA (1978), pp. 102.
[15] M. S. Leu, T. S. Chin, MRS Symp. Proc. **577**, 577 (1999).